High-Energy Emissions induced by air density fluctuations of discharges

Köhn, C.; Chanrion, O.; Neubert, T.

Published in:
Geophysical Research Letters

Link to article, DOI:
10.1029/2018GL077788

Publication date:
2018

Document Version
Peer reviewed version

High Energy Emissions induced by air density fluctuations of discharges

C. Köhn[1], O. Chanrion[1], and T. Neubert[1]

C. Köhn, koehn@space.dtu.dk

[1]Technical University of Denmark,

National Space Institute (DTU Space),

Elektrovej 328, 2800 Kgs Lyngby, Denmark

This article has been accepted for publication and undergone full peer review but has not been through the copyediting, typesetting, pagination and proofreading process, which may lead to differences between this version and the Version of Record. Please cite this article as doi: 10.1029/2018GL077788

Bursts of X- and γ-rays are observed from lightning and laboratory sparks. They are bremsstrahlung from energetic electrons interacting with neutral air molecules, but it is still unclear how the electrons achieve the required energies. It has been proposed that the enhanced electric field of streamers, found in the corona of leader tips, may account for the acceleration, however, their efficiency is questioned because of the relatively low production rate found in simulations. Here we emphasize that streamers usually are simulated with the assumption of homogeneous gas, which may not be the case on the small temporal and spatial scales of discharges. Since the streamer properties strongly depend on the reduced electric field E/n, where n is the neutral number density, fluctuations may potentially have a significant effect. To explore what might be expected if the assumption of homogeneity is relaxed, we conducted simple numerical experiments based on simulations of streamers in a neutral gas with a radial gradient in the neutral density, assumed to be created, for instance, by a previous spark. We also studied the effects of background electron density from previous discharges. We find that X- and γ-radiation is enhanced when the on-axis air density is reduced by more than 25%. Pre-ionization tends to reduce the streamer field and thereby the production rate of high-energy electrons, however, the reduction is modest. The simulations suggest that fluctuations in the neutral densities, on the temporal and spacial scales of streamers, may be important for electron acceleration and bremsstrahlung radiation.

Keypoints:

- Air perturbations significantly increase the velocity of streamer fronts.
- Air perturbations facilitate the emission of X-rays from streamer discharges.
- Preionization moderately lowers the maximum energy of electrons and photons.

1. Introduction

Terrestrial gamma-ray Flashes (TGFs) are photon bursts with energies of up to 40 MeV originating from thunderstorms. They were first observed in 1994 from the Compton Gamma-ray Observatory satellite [*Fishman et al.* , 1994] and later confirmed by other space-based observations [*Smith et al.* , 2005; *Briggs et al.* , 2010; *Marisaldi et al.* , 2010]. X-rays have also been observed at closer proximity to the source with sensors on the ground and on balloons [*Moore et al.* , 2001; *Dwyer* , 2004; *Mallick et al.* , 2012], and in high-voltage laboratory discharge experiments of long sparks [*Dwyer et al.* , 2005; *Babich et al.* , 2015; *Kochkin et al.* , 2014, 2016]. The X- and γ-rays are produced by high-energy, runaway electrons through the bremsstrahlung process, however, the acceleration process of these electrons is still under debate.

There are currently two theories explaining the origin of TGFs. One is that seed electrons from cosmic ray ionization of the atmosphere are born with energies in the runaway regime and are further accelerated by the ambient electric field in a cloud, forming a relativistic runaway electron avalanche (RREA) [*Wilson* , 1925; *Gurevich et al.* , 1992; *Dwyer* , 2003; *Babich et al.* , 2012; *Gurevich and Karashtin* , 2013] including the feedback mechanism where high-energy electrons produce high-energy gamma rays through the bremsstrahlung process which subsequently produce secondary electrons and positrons through photoionization, Compton scattering or pair production [*Dwyer* , 2003, 2007; *Kutsyk et al.* , 2011; *Skeltved et al.* , 2014]. The other is that thermal (cold) electrons are accelerated into the runaway regime in the high, but very localized, field of streamer tips as well as by the enhanced electric fields in the vicinity of lightning leader tips [*Chan-*

rion and Neubert , 2008; *Celestin and Pasko* , 2011; *Babich et al.* , 2015; *Köhn et al.* , 2014, 2015, 2017a] and subsequently turn into relativistic run-away electron avalanches [*Moss et al.* , 2006; *Carlson et al.* , 2010; *Köhn et al.* , 2017a]. In the following we explore the streamer mechanism.

Lightning leaders propagate by means of a multitude of streamers. Streamers are ionization waves formed when the avalanche of thermal electrons create space charge fields of magnitudes that approach the levels of the background field [*Raizer* , Springer-Verlag, Berlin, Heidelberg, 1991].

Past models of electron acceleration by streamers suggest that runaway electrons are created in the high-field region of the streamer tips [*Babich et al.* , 2015; *Chanrion and Neubert* , 2010; *Celestin and Pasko* , 2011], and that these are further accelerated in the larger-scale leader field to flux levels that can account for TGF observations [*Dwyer et al.* , 2008; *Briggs et al.* , 2011]. However, the environment of the leader tip is very complex and to a large extent unknown, and there are currently no self-consistent models that account for the leader-streamer interaction and propagation of the leader, at least not on a plasma kinetic level. Early discussions of density perturbations in connection with discharges suggest that, before the formation of a hot conductive leader channel, streamers heat the air and induce a radial flow of neutral air molecules, which reduces the air density in the streamer path by up to 50% [*Marode et al.* , 1979]. Similar conclusions were reached for positive streamers in a point-plane electrode geometry in the more recent simulations of *Eichwald* [1998]; *Kacem et al.* [2013]; *Eichwald et al.* [2011]; *Ono et al.* [2004]; *Liu and Zhang* [2014]. Tholin and Bourdon simulated the hydrodynamic air expansion

from a nanosecond pulsed spark discharges in a point-to-point gap of 2.5 mm length and for a voltage pulse peaked at approximately 5 kV, hence in a maximum ambient field of approximately 20 kV cm^{-1} plate-electrodes equivalent [*Tholin and Bourdon* , 2013]. Under such conditions, they found that spark discharges initiate pressure waves potentially decreasing the air density by a factor of 50%. By coupling the fluid equations of discharge dynamics and the hydrodynamic equations for the air flow, Agnihotri et al. observed that ambient air heats up to approx. 800 K within tens of nanoseconds within a mean ambient field of 17 kV cm^{-1}. This heating process and the induced pressure waves are effective enough to initiate electrical breakdown without the streamer mechanism with locally enhanced electric field tips [*Agnihotri et al.* , 2017]. Beyond air perturbations induced by shock waves and heating processes, civil transport aircrafts, high-speed air vehicles or the wind flow around (sharp) objects [*Fleming et al.* , 2001; *Gumbel* , 2001; *Lawson and Barakos* , 2011; *Gu et al.* , 2012; *Corda* , 2017] can initiate large pressure and thus air density gradients. The efficiency of the streamer discharge mechanism under more realistic conditions is therefore unclear (see for example discussions in [*Dwyer et al.* , 2012]).

Here we take a step towards a more realistic scenario where the neutral density is considered inhomogeneous on spatial and temporal scales of streamers, as in the environment of a propagating leader tip. We imagine a multitude of streamers emitted from a leader tip, facilitating the leader propagation, and that filaments of neutral density depletion are created in the stepping process from heating of the neutral gas. We consider a scenario that can be accommodated in our model, whereby a streamer is propagating along the

axis of a filament. In previous work, we have discussed air perturbations as well as their origin and focused on streamer properties in inhomogeneous air [*Köhn et al.* , 2018]. Conclusively, we found that the streamer velocities as well as the streamer morphology depend on the spatial distribution of ambient air. Depending on the perturbation level, electrons reach energies of up to several keV suggesting the production of X-rays in perturbed air. We here now continue and explore the possible effect of air perturbations on the emission of X-rays from streamer discharges.

Temporal and spatial scales of discharges, and the magnitude of the threshold electric field E, are inversely proportional to the neutral density, n, and perturbations to the neutral density could therefore potentially affect the streamer properties. The reduced electric field, E/n is often used when discussing discharge processes. In air at standard temperature and pressure, with a homogeneous density and electric field, the reduced breakdown field, E_k/n is ≈ 125 Td corresponding to $E_k = 3.2$ MVm^{-1} at standard temperature and pressure where $n = 2.55 \cdot 10^{25}\mathrm{m}^{-3}$.

In the following we present proof-of-concept simulations that explore the impact of streamer-scale inhomogeneities on electron acceleration and bremsstrahlung radiation. Our model does not self-consistently account for air perturbations, but is meant to identify the possible effects on streamers that may be induced by density perturbations, an area that that until now is largely unexplored.

2. Methods

Following *Babich et al.* [2015], we hypothesize simple radial profiles of air and electron densities of channels formed by preceding streamers and compare with results obtained in uniform air without pre-ionization.

2.1. Set-up of the model

The computational model is based on a 2.5D cylindrically symmetric Particle-In-Cell, Monte Carlo code with adaptive super-particles representing w real particles. An adaptive particle scheme can change the weight (w) and number of super electrons while conserving the energy, momentum and the charge distribution [*Chanrion and Neubert* , 2008]. It allows us to increase the resolution of high-energy particles (w small) and to reduce the computational load of the large amount of low-energy electrons (max 100 particles in a cell). The code has two spatial (r, z) and three velocity coordinates (v_r, v_θ, v_z). The simulation domain is $L_r = 1.25$ mm in the r-direction and $L_z = 14$ mm in the z-direction with a mesh of 150×1200 grid points. Since we use a particle code, updating the position of electrons and photons, as well as accounting for the collisions with air molecules, is independent of the actual grid. The grid is used to solve Poisson's equation for the electrostatic potential, ϕ, from the particle charge distributions after every time step. The air density is unaffected by the streamer and remains constant during a simulation. The ions are immobile at the location of their creation and only the electrons are accelerated by the local electric field. The interactions of electrons with the neutral molecules include ionization, elastic and inelastic scattering, attachment and detachment as well as bremsstrahlung emissions [*Chanrion and Neubert* , 2008; *Köhn and Ebert* , 2014].

In all simulations, the ambient electric field, E_{amb}, is 1.5 E_k where E_k is the breakdown field in unperturbed air. At the boundary $(r = 0, L_r)$ we use the Neumann condition for the electric potential, $\partial\phi/\partial r = 0$, and at $(z = 0, L_z)$ the Dirichlet conditions $\phi(r, 0) = 0$ and $\phi(r, L_z) = E_{amb}L_z$. As in [*Chanrion and Neubert* , 2008; *Köhn et al.* , 2017b] we initiate the streamer with a Gaussian electron-ion patch with a peak density of 10^{20} m^{-3}, a width of 0.2 mm and centered at $z_0 = 7$ mm. The patch is charge neutral at $t = 0$.

2.2. Air density perturbations

We model the effects of small-scale air density perturbations and ionization by a preceding streamer as suggested in [*Hill and Robb* , 1968; *Plooster* , 1970; *Marode et al.* , 1979; *Eichwald et al.* , 1996; *Gonzalez et al.* , 2001; *Villagrán-Muniz et al.* , 2003; *Kacem et al.* , 2013; *Liu and Zhang* , 2014; *Babich et al.* , 2015]. We choose sinusoidal air density perturbation in the radial direction with the minimum on the axis $(r = 0)$ and the maximum at the outer boundary $(r = L_r)$:

$$n_j(r) = n_0 \left(1 - \xi_j \cos(r\pi/L_r)\right); j = 0, 4 \tag{1}$$

where $n_0 = 2.55 \cdot 10^{25}$ m^{-3} is the background neutral density at sea level and $\xi_{j=0-4}$, is the perturbation amplitude of the j'th profile simulated. We consider the following levels of perturbations: $\xi_j = 0, 0.25, 0.5, 0.75, 1.0$, which represent differences on the r-axis of 0% to 100%. We note here that the ratio E_{amb}/E_k depends on r for $j > 0$. For example for $j = 3$, $E_{amb}(0, z)/E_k = 6$, $E_{amb}(L_r/2, z)/E_k = 1.5$ and $E_{amb}(L_r, z)/E_k = 0.86$. Hence, the effective electric field is strongly enhanced only in a small region around the symmetry axis. Various measurements have shown that electric fields in streamer discharges can

reach field strengths of up to $\approx 10E_k$[*Spyrou and Manassis* , 1989; *Pancheshyi et al.* , 2000; *Kim et al.* , 2004] consistent with results of streamer simulations and analytic estimates [*Liu and Pasko* , 2004; *Moss et al.* , 2006; *Chanrion and Neubert* , 2008; *Naidis* , 2009; *Tholin and Bourdon* , 2013; *Qin and Pasko* , 2014; *Köhn et al.* , 2018]. In the vicinity of lightning leader tips, calculations have shown that the enhanced electric field can exceed several times the breakdown field [*Köhn et al.* , 2015, 2017a].

In an electric field of $6E_k$, the ionization length $1/\alpha_{ion}(E)$, where $\alpha_{ion}(E)$ is the Townsend coefficient [*Chanrion and Neubert* , 2008], is 3 μm whilst the ionization length amounts to approx. 111 μm in a field of $0.86E_k$. Thus, on the boundaries $r = 0$ and $r = L_r$, the ionization length is small enough to allow the formation of streamers, yet significantly different such that electrons experience the effect of non-uniform air. We here note that the case $j = 4$ is an extreme case which we use to conclude our parameter study extrapolating perturbations of 80% and above. The functional shape of the density is meant to capture the scale, the density minima and the radial gradients of the perturbations. Other than that, the function chosen is not important for our conclusions.

2.3. Pre-ionization

In order to address the impact of pre-ionization, we simulate conditions without pre-ionization and with pre-ionization $n_{e,0} = 10^{12}$ m^{-3} as used by *Babich et al.* [2015] and also used in [*Nijdam et al.* , 2011]. Other simulations [*Köhn et al.* , 2017c, 2018] indicate that the electron density in the streamer channel left behind is in the order of $10^{16} - 10^{20}$ m^{-3}.

After a discharge, the time of field screening inside the previous channel is determined by the times for electron attachment and ion-ion recombination. The time of electron attachment in air is

$$t_{att} = 1/(k_{att} \cdot (n_{O_2})^2) \tag{2}$$

with the oxygen density $n_{O_2} = 0.2n$, air density n and with $k_{att} = 2 \cdot 10^{-30}$ cm^6 s^{-1} [*Kossyi et al.* , 1992]. After electron attachment, the time of ion-ion recombination is calculated through

$$t_{rec} = 1/\left((k_{rec,1} + k_{rec,2} \cdot n) \cdot n\right) \tag{3}$$

with $k_{rec,1} = 10^{-7}$ cm^3 s^{-1} and $k_{rec,2} = 2 \cdot 10^{-25}$ cm^6 s^{-1} [*Pancheshnyi et al.* , 2005]. For $n = n_0$, it is $t_{att} = 20$ ns and $t_{rec} \approx 7.8$ fs; for $n = 0.1n_0$, it is $t_{att} = 2$ μs and $t_{rec} \approx 0.7$ ps. As we will discuss in section 4, the life time of air perturbations is in the order of 50 ms, thus significantly larger than the time to readjust the electric field.

The electric field will diffuse within time $\tau_{diff} \simeq \nu_{en}/\omega_{pe}^2$ [*Banks et al.* , 1990; *Neubert et al.* , 1996] where ν_{en} is the collision frequency of electrons and ω_{pe} the plasma frequency. If we approximate the maximum collision frequency at standard temperature and pressure $\nu_{en} \approx 8.45 \cdot 10^{12}$ s^{-1}, and noting that the plasma frequency ω_{pe} ranges from $5.65 \cdot 10^7$ s^{-1} up to $5.65 \cdot 10^{11}$ s^{-1} for pre-ionization levels of $10^{12} - 10^{20}$ m^{-3}, the electric field diffusion time becomes $\tau_{diff} = 26.52$ ps–2.65 ms. Thus, for levels of preionization $\lesssim 10^{16}$ m^{-3} $\tau_{diff} > 100$ ns, is longer than the time scale for air perturbations [*Marode et al.* , 1979] or the time scale for streamer simulations at sea-level [*Köhn et al.* , 2017c, 2018]. For the field to re-establish itself within a previous streamer body, we must place an additional assumption that either the time between the old streamer and the new streamer is longer

than these time constants or that a new potential wave is propagating into the streamer body from the leader tip as discussed by *Bazelyan and Raizer* [2000]; *Babich et al.* [2015].

3. Results

3.1. Temporal evolution of the electron density

The electron densities, n_e, of the streamers without pre-ionization are shown in Figure 1 (a-h). To ease comparison with the unperturbed case, which is usually considered in simulations of streamers, the left halves are for unperturbed air, j=0, and the right halves for j=1 to 4. We have chosen to show the results at three times, determined by the maximum time that can be accommodated in the simulation domain. For the two smaller perturbation levels the simulations can run longer because the streamers develop and propagate slower ($t = 1.03$ ns), and for the two higher perturbation levels we must stop the simulations earlier because the streamers develop rapidly in the low density regions ($t = 0.37$ ns for $\xi_j = 0.75$ and $t = 0.12$ ns for $\xi_j = 1.0$). As supplementary material we have added the temporal evolution of this comparison. In order to compare the streamer evolution at the same time step, panels (e-h) show the electron density for all cases after 0.12 ns.

The ambient electric field is pointing downwards such that positive streamers propagate downwards and negative streamers upwards. Panels (a-h) show that for small perturbations, below 50%, the positive and negative streamer fronts both develop and propagate almost with the same pattern as in unperturbed air, although faster with increasing ξ_j. For high levels of perturbations, the negative streamer develops and propagates faster than the positive and it becomes difficult to identify a positive front. The differences in their

properties come from the underlying mechanisms of their propagation. Negative streamers are primarily driven by electron impact ionization as they propagate in the same direction as electrons are accelerated (against the field), whereas positive streamers primarily propagate by means of photo ionization of O_2 from excitation of N_2 by electrons accelerated ahead of the streamer and against its direction of propagation (e.g. [*Zheleznyak et al.* , 1982]). For the high values of ξ_j, the reduced density of air molecules reduces the production of photo electrons important for the positive streamers and increases the mean free path of electron ionization, allowing electrons to move longer distances and achieve higher energies between collisions in the negative streamers.

The changes in streamer formation and acceleration in perturbed air is illustrated by considering the mean velocities of streamers. Because the streamers continue to accelerate at the end of the simulations and we stop the simulations at different times, it is not meaningful to calculate and compare the velocities themselves. Rather, we determine the mean streamer velocities in perturbed air normalized to the corresponding unperturbed velocities. Since we stop the simulations for perturbation levels of 75% and 100% within 1 ns, it is hard to identify clear positive fronts and hence we are not able to determine normalized velocities of positive streamers in these cases. The mean velocities are calculate from the position of the fronts at $t = 0.01$ ns and t_{end}. The results are shown in Table 1. We find that normalized velocities of both polarities increase with increased level of perturbation reaching $\simeq$70 for the negative polarity at $\xi = 1$. This is consistent with experiments [*Briels et al.* , 2008], theoretical considerations [*Ebert et al.* , 2010] and numerical simulations [*Liu and Pasko* , 2004; *Pancheshnyi et al.* , 2005] showing that

positive and negative streamers move faster for higher so-called reduced fields, i.e. higher electric fields for fixed air density or for reduced air density in a constant electric field.

Fig. 1 i) - l) illustrates the importance of pre-ionization on the temporal evolution of the electron density for the same perturbation levels and time steps as in panels a) - d). The left half of each panel shows the electron density with a pre-ionization level of 10^{12} m^{-3} and the right half without pre-ionization, hence as the right halves of panels a)-d). Additionally, Table 1 compares the velocities of the streamer fronts without and with pre-ionization. In all considered cases, the streamer fronts move slower in the presence of pre-ionization [*Nijdam et al.* , 2011] for the same ξ_j, but still faster than streamers in uniform air. However, the effect of streamers being faster than in uniform air, increasing with ξ_j, is still prevalent in the presence of pre-ionization.

3.2. Occurrence of high-energy electrons and X-rays

The energy distributions of electrons at the end of the simulations are shown in Figure 2. The distributions in unperturbed air are shown as reference (solid curves) together with the distributions in perturbed air without pre-ionization (dashed lines) and with pre-ionization (circles). The distributions of bremsstrahlung photons in perturbed air are shown without pre-ionization (crosses) and with pre-ionization (squares). We see that, as expected, the number of electrons and the maximum electron energy increases with the perturbation level. The maximum electron energies for ξ_{2-4}, reached at the end of the simulations, are approximately 200 eV (200 eV with pre-ionization), 3 keV (1 keV) and 100 keV (50 keV) after 1.03 ns, 0.37 ns and 0.12 ns. In comparison, the maximum electron energies in uniform air are $\approx$ 100 eV, which is agreement with earlier results of electron

energies of streamer discharges in perturbed air [*Köhn et al.* , 2018]. The higher energies are caused by the higher reduced electric field close to the axis, which allows for stronger electron acceleration. For perturbations of 75% and 100%, the generation rate of runaway electrons above 1 keV is approximately $3.8 \cdot 10^{12}$ s^{-1} and $3.4 \cdot 10^{17}$ s^{-1}, respectively. *Schaal et al.* [2012] performed ground-based observations of high-energy emission from natural and rocket-triggered lightning and subsequently estimated the generation rate of energetic electrons producing X-rays. They found rates of approximately 10^{12} s^{-1} - 10^{17} s^{-1} which agrees very well with our simulation results.

In the cases of pre-ionization, the electron number densities are reduced for ξ_{3-4} because the pre-ionization space charge tends to reduce the field, however, the reduction is modest and of the order of a factor 2. The reduction in the maximum electron energy is more significant caused by a lower acceleration of electrons. In such a configuration, the generation rate of electrons above 1 keV is $0.4 \cdot 10^{12}$ s^{-1} for $\xi_3 = 0.75$ and $0.1 \cdot 10^{17}$ s^{-1} for $\xi_4 = 1.0$ which is smaller than without pre-ionization, but still in the range determined by *Schaal et al.* [2012].

We also observe the occurrence of photons at the higher perturbation levels, ξ_{2-4}. Their production is a direct consequence of the existence of energetic electrons. After the acceleration of electrons in the low-density region, the local electric field at the streamer head moves some electrons to higher-density regions where they create X-rays through the bremsstrahlung process. The energy and number density of photons reflect the properties of the electrons. The lower density of energetic electrons for n_3 suppresses the photon distribution to just a few photons. The maximum photon energy is 3 keV without and 400

eV with pre-ionization. For n_4, on the other hand, the difference in the photon spectra is modest; the maximum photon energy in this case is 30 keV without and 15 keV with pre-ionization. This difference is caused by the sensitivity of the spectra to the time the simulations are stopped, affecting the case of n_3 more strongly because the high energy tail of electrons has not had time to fully develop in this case. The results suggest, therefore, that the amplitude of the bremsstrahlung photon spectra for pre-ionization is modified similar to that of electrons, i.e. by a factor ~ 2. The maximum energy of electrons, ϵ_e, and photons, ϵ_γ, as well as the photon number N_γ with and without pre-ionization are shown in Table (1).

4. Discussion and outlook

Discussing the influence of air perturbations on the production of X- and γ-rays from electric discharges, we have to distinguish the effects of streamers from that of leaders. In laboratory experiments of long discharges [*Kochkin et al.* , 2012, 2014], multiple streamers propagate in close proximity to each other and experiments have shown that X-rays occur within tens of ns when multiple streamers are concentrated in a small volume around the electrode. The observed currents at the grounded electrode and the high-voltage electrode during the production of X-rays in these experiments is in the order of 100 A . The work of *Marode et al.* [1979] shows that streamers with peak currents of several hundreds of mA perturb air by a factor of 50% in a radius of several μm within tens of ns. Hence, the effect of density perturbations from bypassing streamers is not negligible and can influence the properties of neighboring streamers. The lifetime of the perturbations in the streamer corona is in the order of $L_r^2/D_{air} \simeq 50$ ms with a diffusion coefficient

$D_{air} \simeq 2 \cdot 10^{-5}$ m^{2}s^{-1} [*Cussler* , 1997]. This is large enough for following streamers to encounter inhomogeneities created by preceding streamers. For instance, it is observed both in lightning of the atmosphere, and for sprites in the mesosphere, that streamers may follow paths created by earlier streamers [*Nijdam et al.* , 2014]. In addition, spherical and cylindrical shock waves associated with lightning leader propagation create large over-pressures such that the air density in its vicinity is reduced up to 100% [*Plooster* , 1970; *Liu and Zhang* , 2014]. There is no doubt, therefore, that the environment around leader tips is complex, highly inhomogeneous and dynamic. We have shown for the rather simple case of perturbations from a single streamer filament perturbation that such environment it is likely to enhance electron acceleration and bremsstrahlung radiation from streamers relative to a homogeneous air.

Our simulations suggest that inhomogeneities in the background air density, resulting from streamers ahead of lightning leaders, from shock waves associated with lightning leaders or from neighboring streamers simultaneously propagating close to each other, may have a profound effect on electron acceleration and bremsstrahlung radiations in streamers. There are two simultaneous effects at play which are not present in uniform air. One is that electrons can gain high energies in the center regions of streamers where the air density is reduced and the other is that at the air density is high at the edge of the streamers allowing high electric fields to be established in the ionization wave. Thus our results suggest the thermal acceleration mechanism may play a role as a source of energetic radiation as observed from lightning and laboratory sparks.

Table 1 shows the number of photons produced ranges between 3 and about 22000 within 0.12 to 1.03 ns depending on the perturbation level and the existence of pre-ionization. For comparison, the total number of photons in a TGF is estimated from satellite observations to be in the range of $\approx 10^{11} - 10^{18}$ photons with energies between several keV to tens of MeV, with the lower photon number limit determined by the instrument sensitivities [*Gjesteland et al.* , 2010; *Østgaard et al.* , 2015]. If the streamer zone of a lightning leader tip consists of approx. 10^6 streamers as assumed by *Celestin and Pasko* [2011], the average production of one streamer is $\approx 10^5 - 10^{12}$ photons above 1 keV. Both the photon energies and the number of photons in TGFs are then much higher than obtained in our simulations. We point out, though, that our simulations are stopped very early because of the limitations on the simulation domain size. Subsequently, we miss the initiation of a relativistic run-away electron avalanche (RREA) and thus a further amplification of the number of high-energy electrons. We can then only conclude that density perturbations enhance the number of relativistic electrons and significantly increase the photon flux relative to the unperturbed case.

In laboratory experiments, on the other hand, the estimated number of photons produced in a discharge was $10^3 - 10^4$ [*Kochkin et al.* , 2016; *Nguyen et al.* , 2008] and the estimated number of photons being produced by one single streamer $2 \cdot 10^{-3}$ [*Nguyen et al.* , 2010].

Hence, the average number of photons produced by single streamer discharges ranges from $10^5 - 10^{12}$ photons for TGFs till $\lesssim 1$ photon for X-rays measured in laboratory

discharges. For perturbation levels of 75% or 100% we observe 777 photons (9 with pre-ionization) or 21816 (5247), respectively, which lies in-between this number range.

Laboratory discharges likely have lower photon energies and photon numbers in a discharge relative to naturally occurring TGFs because of the limited size of laboratory experiments and of the energy of a discharge. Because of computational limitations, the simulations presented in this manuscript are performed in a small spatial domain. In this way, the laboratory setting is closer to our simulation scenario. In order to improve our understanding of the role of density perturbations in facilitating the production of TGFs, it would be desirable to run further simulations in a larger domain for several ms instead of ns as well as to treat air perturbations self-consistently accompanying the electron motion, the streamer development and the emission of X-rays. However, as computational costs are currently too high, we conclude then, that radiation enhanced by density perturbations is a likely candidate accounting for radiation in high-voltage experiments giving us a hint about the production of TGFs in perturbed air, and we point out that future, more realistic, simulations of streamer discharges and the associated emission of X-rays potentially need to involve the gas dynamics of ambient air.

Acknowledgments. We would like to thank Ute Ebert from the Centrum voor wiskunde en informatica (CWI), Amsterdam, the Netherlands, for fruitful discussions to improve the paper. The research was partly funded by the Marie Curie Actions of the European Union's Seventh Framework Programme (FP7/2007-2013) under REA grant agreement nº 609405 (COFUNDPostdocDTU). The work presented was developed in the framework of the TEA-IS network of the European Science Foundation.

The data used for this publication can be obtained from DOI:10.5281/zenodo.1228095.

References

Agnihotri, A., Hundsdorfer, W., and Ebert, U. (2017). Modeling heat dominated electric breakdown in air with adaptivity to electron or ion time scales. *Plasma Sour. Sci. Technol.* 26, 095003.

Babich, L.P., Bochkov, E.I., Dwyer J.R., and Kutsyk, I.M. (2012). Numerical simulations of local thundercloud field enhancements caused by runaway avalanches seeded by cosmic rays and their role in lightning initiation. *J. Geophys. Res.* 117, A09316.

Babich, L.P., Bochkov, E.I., Kutsyk, I.M., Neubert, T., and Chanrion, O. (2015). A model for electric field enhancement in lightning leader tips to levels allowing X- and γ-ray emissions. *J. Geophys. Res. Space Phys.* 120, 5087–5100.

Banks, P.M., Fraser-Smith, A.C., and Gilchrist, B.E. (1990). Ionospheric modification using realistic electron beams. *AGARD Conference Proceedings* 485, 22.

Bazelyan, E.M., and Raizer, Y.P. (2000). Lightning physics and lightning protection. *IOP Publishing* Bristol, England.

Briels, T.M.P., Kos, J., Winands, G.J.J., van Veldhuizen, E.M., and Ebert, U. (2008). Positive and negative streamers in ambient air: measuring diameter, velocity and dissipated energy. *J. Phys. D: Appl. Phys.* 41, 234004.

Briggs, M.S., et al. (2010). First result on terrestrial gamma ray flashes from the Fermi Gamma-ray Burst Monitor. *J. Geophys. Res.* 115, A07323.

Briggs, M.S., et al. (2011). Electron-positron beams from terrestrial lightning observed with Fermi GBM. *Geophys. Res. Lett.* 38. L02808.

Carlson, B.E., Lehtinen, L.G., and Inan, U.S. (2010). Terrestrial gamma ray flash production by active lightning leader channels. *J.* Geophys. Res. 115, A10324.

Celestin, S., and Pasko, V.P. (2011). Energy and fluxes of thermal runaway electrons produced by exponential growth of streamers during the stepping of lightning leaders. *J. Geophys. Res.* 116, A03315.

Chanrion, O., and Neubert, T. (2008). A PIC-MCC code for simulation of streamer propagation in air. *J. Comp. Phys.* 227, 7222–7245.

Chanrion, O., and Neubert, T. (2010). Production of runaway electrons by negative streamer discharges. *J. Geophys. Res.* 115, A00E32.

Corda, S. (2017). *Introduction to Aerospace Engineering with a Flight Test Perspective* (J. Wiley & Sons Ltd., West Sussex, United Kingdom).

Cussler, E.L. (1997). Diffusion: Mass Transfer in Fluid Systems. *Cambridge University Press,* New York.

Dwyer, J.R. (2003). A fundamental limit on electric fields in air. *Geophys. Res. Lett.* 30, 2055.

Dwyer, J.R., Rassoul, H.K., Saleh, Z., Uman, M.A., Jerauld, J., and Plumer, J.A. (2005). X-ray bursts produced by laboratory sparks in air. *Geophys. Res. Lett.* 32, L20809.

Dwyer, J.R. (2004). Implications of X-ray emissions from lightning. *Geophys. Res. Lett.* 31, L12012.

Dwyer, J.R. (2007). Relativistic breakdown in planetary atmospheres. *Phys. of Plasmas* 14, 042901.

Dwyer, J.R., Grefenstette, B.W., and Smith, D.M. (2008). High-energy electron beams launched into space by thunderstorms. *Geophys. Res. Lett.* 35, L02815.

Dwyer, J.R., Smith, D.M., and Cummer, S.A. (2012). High-energy atmospheric physics: Terrestrial Gamma-ray Flashes and related phenomena. *Space Sci. Rev.* 173, 133–196.

Ebert, U., et al. (2010). Review of recent results on streamer discharges and discussion of their relevance for sprites and lightning. *J. Geophys. Res.* 115, A00E43.

Eichwald, O., Jugroot, M., Bayle, P., and Yousif, M. (1996). Modeling neutral dynamics in pulsed helium short-gap spark discharges. *J. Appl. Phys.* 80, 694–709.

Eichwald, O., Yousfi, Y., Bayle, P., and Jugroot, M. (1998). Modeling and threedimensional simulation of the neutral dynamics in an air discharge confined in a microcavity. I. Formation and free expansion of the pressure waves. *J. Appl. Phys.* 84, 4704.

Eichwald, O., Yousfi, Y., Ducasse, O., Merbahi, N., Sarrette, J.P., Meziane, M., and Benhenni, M. (2011). Electro-hydrodynamics of micro-discharges in gases at atmospheric pressure. *Hydrodynamics - Advanced topics* edited by Schulz, H.E., et al. ISBN: 978-953-307-596-9, InTech, DOI:10.5772/2372.

Fishman, G.J., et al. (1994). Discovery of intense gamma-ray flashes of atmospheric origin. *Science* 264, 1313–1316.

Fleming, E.F., Jackman, C.H., Considine, D.B., and Stolarski, R.S. (2001). Sensitivity of tracers and a stratospheric aircraft perturbation to two-dimensional model transport variations. *J. Geophys. Res. Atmos.* 106, 14245–14263.

Gjesteland, T., Østgaard, N., Connell, P.H., Stadsnes, J., and Fishman, G.J. (2010). Effects of dead time losses on terrestrial gamma ray flash measurements with the Burst

and Transient Source Experiments. *J. Geophys. Res.* 115, A00E21.

Navarro-Gonzalez, R., Villagrán-Muniz, M., Sobral, H., Molina, L.T., and Molina M.J. (2001). The physical mechanism of nitric oxide formation in simulated lightning. *Geophys. Res. Lett.* 28, 3867–3870.

Gu, A., and Lim, H.C. (2012). Wind flow around rectangular obstacles and the effects of aspect ratio. *The seventh international colloquium on bluff body aerodynamics and applications* 244–253.

Gumbel, J. (2001). *J. Geophys. Res.* 106, 10553–10563.

Gurevich, A.V., Milikh, G., and Roussel-Dupré, R. (1992). Runaway electron mechanism of air breakdown and preconditioning during a thunderstorm. *Phys. Lett. A* 165, 465–468.

Gurevich, A.V., and Karashtin, A.N. (2013). Runaway breakdown and hydrometeors in lightning initiation. *Phys. Rev. Lett.* 110, 185005.

Hill, E.L., and Robb, J.D. (1968). *J. Geophys. Res.* 73, 1883–1888.

Kacem, S., et al. (2013). Simulation of expansion of thermal shock and pressure waves induced by a streamer dynamics in positive DC corona discharges. *IEEE Trans. Plasma Sci.* 41, 942–947.

Kim, Y., Kang, W.S., Park, J.M., Hong, S.H., Song, Y.H., and Kim, J. (2004). Experimental and numerical analysis of streamers in pulsed corona and dielectric barrier discharges. *IEEE Trans. Plasma Sci.* 32, 18–24.

Kochkin, P.O., Nguyen, C.V., van Deursen, A.P.J., and Ebert, U. (2012). Experimental study of hard x-rays emitted from metre-scale positive discharges in air. *J. Phys. D:*

Appl. Phys. 45, 425202.

Kochkin, P.O., van Deursen, A.P.J., and Ebert, U. (2014). Experimental study of the spatio-temporal development of metre-scale negative discharge in air. *J. Phys. D Appl. Phys.* 47, 145203.

Kochkin, P.O., Köhn, C., van Deursen, A.P.J., and Ebert, U. (2016). Analyzing X-ray emissions from meter-scale negative discharges in ambient air. *Plasma Sour. Sci. Technol.* 25, 044002.

Köhn, C., and Ebert, U. (2014). Angular distribution of bremsstrahlung photons of positrons for calculations of terrestrial gamma-ray flashes and positron beams. *Atmos. Res.* 135-136, 432–465.

Köhn, C., Ebert, U., and Mangiarotti, A. (2014). The importance of electron-electron Bremsstrahlung for terrestrial gamma-ray flashes, electron beams and electron-positron beams. *J. Phys. D. Appl. Phys. FTC* 47, 252001.

Köhn, C., and Ebert, U. (2015). Calculation of beams of positrons, neutrons, and protons associated with terrestrial gamma ray flashes. *J. Geophys. Res.* 120, 1620–1635.

Köhn, C., Diniz, G., and Harakeh, M.N. (2017a). Production mechanisms of leptons, photons and hadrons and their possible feedback close to lightning leaders. *J. Geophys. Res.* 112, 1365–1383.

Köhn, C., Chanrion, O., and Neubert, T. (2017b). The influence of Bremsstrahlung on electric discharge streamers in N_2, O_2 gas mixtures. *Plasma Sour. Sci. Technol.* 26, 015006.

Köhn, C., Chanrion, O., and Neubert, T. (2017c). Electron acceleration during streamer collisions in air. *Geophys. Res. Lett.* 44, 2604–2614.

Köhn, C., Chanrion, O., Babich, L.P., and Neubert, T. (2018). Streamer properties and associated X-rays in perturbed air. *Plasma Sour. Sci. Technol.* 27, 015017.

Kossyi, I.A., Kostinsky, A.Y., Matveyev, A.A., and Silakov, V.P. (1992). Kinetic scheme of the non-equilibrium discharge in nitrogen-oxygen mixtures. *P*lasma Sour. Sci. Technol. 1 207.

Kutsyk, I.M., et al. (2011). Self-sustained relativistic-runaway-electron avalanches in the transverse field of lightning leader as sources of terrestrial gamma-ray flashes. *E.N. Jetp Lett.* 94, 606.

Lawson, S.J., and Barakos, G.N. (2011). Review of numerical simulations for high-speed, turbulent cavity flows. *Progress Aero. Sci.* 47, 186–216.

Liu, N., and Pasko, V.P. (2004). Effects of photoionization on propagation and branching of positive and negative streamers in sprites. *J. Geophys. Res.* 109, A04301.

Liu, Q., and Zhang, Y. (2014). Shock wave generated by high-energy electric spark discharges. *J. Appl. Phys.* 116, 153302.

Mallick, S., Rakov, V.A., and Dwyer, J.R. (2012). A study of X-ray emissions from thunderstorms with emphasis on subsequent strokes in natural lightning. *J. Geophys. Res.* 212, D16107.

Marisaldi, M., et al. (2010). Detection of terrestrial gamma ray flashes up to 40 MeV by the AGILE satellite. *J. Geophys. Res.* 115, A00E13.

Marode, E., Bastien, F., and Bakker, M. (1979). A model of the streamer included spark formation based on neutral dynamics. *J. Appl. Phys.* 50, 140–146.

Moore, C.B., Eack, K.B., Aulich G.D., and Rison, W. (2001). Energetic radiation associated with lightning stepped-leaders. *Geophys. Res. Lett.* 28, 2141–2144.

Moss, G.D., Pasko, V.P., Liu, N., and Veronis, G. (2006). Monte Carlo model for analysis of thermal runaway electrons in streamer tips in transient luminous event and streamer zones of lightning leaders. *J. Geophys. Res.* 111, A02307.

Naidis, G.V. (2009). Positive and negative streamers in air: Velocity-diameter relation. *Phys. Rev. E* 79, 057401.

Neubert, T., Gilchrist, B., Wilderman, S., Habash, L., and Wang, H.J. (1996). Relativistic electron beam propagation in the earth's atmosphere: modeling results. *Geophys. Res. Lett.* 23, 1009–1012.

Nijdam, S., Wormeester, G., van Veldhuizen, E.M., and Ebert, U. (2011). Probing background ionization: positive streamers with varying pulse repetition rate and with a radioactive admixture. *J. Phys. D: Appl. Phys.* 44, 455201.

Nijdam, S., Takahashi, E., Markosyan, A.H., and Ebert, U. (2014). Investigation of positive streamers by double-pulse experiments, effects of repetition rate and gas mixtures. *Plasma Sour. Sci. Technol.* 23, 025008.

Nguyen, C.V., van Deursen, A.P.J., and Ebert, U. (2008). Multiple x-ray bursts from long discharges in air. *J. Phys. D: Appl. Phys.* 41, 234012.

Nguyen, C.V., van Deursen, A.P.J., van Heesch, E.J.M., Winands, G.J.J., and Pemen, A.J.M. (2010). X-ray emission in streamer-corona plasma. *J. Phys. D: Appl. Phys.* 43,

02502.

Ono, R., and Oda, T. (2004). Visualization of streamer channels and shock waves generated by positive pulsed corona discharges using laser Schlieren method. *Jap. J. Appl. Phys.* 43, 321327.

Østgaard, N., Albrechtsen, K.H., Gjesteland, T., and Collier, A. (2015). A new population of terrestrial gamma-ray flashes in the RHESSI data. *Geophys. Res. Lett.* 42, 10937–10942.

Pancheshnyi, S.V., Sobakin, S.V., Starikovskaya, S.M., and Starkovskii, A.Yu. (2000). Discharge Dynamics and the Production of Active Particles in a Cathode-Directed Streamer. *Plasma Phys. Rep.* 26, 1054–1065.

Pancheshnyi, S., Nudnova, M., and Starikovskii, A. (2005). Development of a cathode-directed streamer discharge in air at different pressures: Experiment and comparison with direct numerical simulation. *Phys. Rev. E* 71, 016407.

Plooster, M.N. (1970). Shock waves from line sources. Numerical solutions and experimental measurements. *Phys. Flu.* 13, 2665–2675.

Qin, J., and Pasko, V.P. (2014). On the propagation of streamers in electrical discharges. *J. Phys. D: Appl. Phys.* 47, 435202.

Raizer, Y.P. (Springer-Verlag, Berlin, Heidelberg, 1991). *Gas Discharge Physics*

Schaal, M.M., Dwyer, J.R., Saleh, Z.H., Rassoul, H.K., Hill, J.D., and Jordan, D.M. (2012). Spatial and energy distributions of X-ray emissions from leaders in natural and rocket triggered lightning. *J. Geophys. Res.* 117, D15201.

Skeltved, B., et al. (2014). Modeling the relativistic runaway electron avalanche and the feedback mechanism with GEANT4. *J. Geophys. Res. Space Phys.* 119, 9174–9191.

Smith, D.M., Lopez, L.L., Lin, R.P., and Barrington-Leigh, C.P. (2005). Terrestrial gamma-ray flashes observed up to 20 MeV. *Science* 307, 1085–1088.

Spyrou, N., and Manassis, C. (1989). Spectroscopic study of a positive streamer in a point-to-plane discharge in air: evaluation of the electric field distribution. *J. Phys. D: Appl. Phys.* 22, 120–128.

Surzhikov, S.T. (2012). Computational Physics of Electric Discharges in Gas Flows. *De Gruyter Studies in Mathematical Physics*.

Tholin, F., and Bourdon, A. (2013). Simulation of the hydrodynamic expansion following a nanosecond pulsed spark discharge in air at atmospheric pressure. *J. Phys. D: Appl. Phys.* 46, 365205.

Villagrán-Muniz, M., Sobral, H., Navarro-Gonzalez, R., Velázquez, P.F., and Raga, A.C. (2003). Experimental simulation of lightning, interacting explosions and astrophysical jets with pulsed lasers. *Plasma Phys. Control. Fusion* 45, 571–584.

Wilson, C. (1925). The electric field of a thundercloud and some of its effects. *Proc. Phys. Soc. Lond.* 37A, 32D–37D.

Zheleznyak, M.B., Mnatsakanian, A.K., and Sizykh, S.V. (1982). Photoionization of nitrogen and oxygen mixtures from a gas discharge. *High Temp.* 20, 357–362.

sidewaystable

Table 1. The mean velocities, $v_j^{\pm}$, and normalized mean velocities $\Xi^{\pm} := (v_j/v_0)^{\pm}$ of negative and of positive streamer fronts at different levels of perturbation (no front is identified for positive streamers for $\xi_{4,5} = 0.75, 1.0$) and the maximum electron and photon energies $\epsilon_e, \epsilon_\gamma$ as well as the photon number N_γ without and with pre-ionization (PI). v_0 is the velocity of the negative and positive streamer front in uniform air.

j	ξ_j	t_{end} [ns]	v_j^+ [mm/ns]	v_j^- [mm/ns]	Ξ^+	Ξ^-	ϵ_e [keV]	ϵ_γ [keV]	N_γ	$v_{j,PI}^+$ [mm/ns]	$v_{j,PI}^-$ [mm/ns]	$\epsilon_{e,PI}$ [keV]	$\epsilon_{\gamma,PI}$ [keV]	$N_{\gamma,PI}$
1	0.25	1.03	0.84	1.39	2.9	1.9	0.2	—	—	0.40	1.00	0.1	—	—
2	0.50	1.03	3.83	4.96	13.2	6.8	0.2	0.1	3	3.28	3.32	0.2	—	—
3	0.75	0.37	—	9.50	—	12.7	3.0	3.0	777	—	5.97	1.0	0.4	9
4	1.00	0.12	—	59.85	—	70.4	100	30	21816	—	59.68	50	15	5247

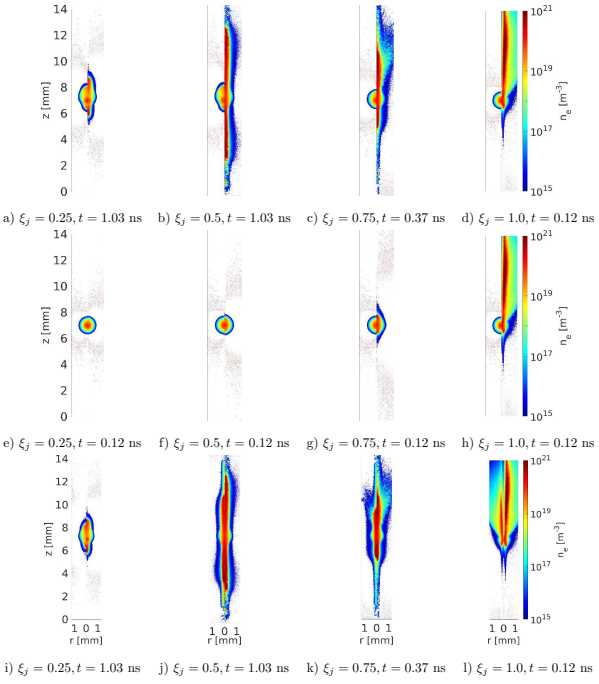

Figure 1. The electron density of streamers for different levels of air density perturbations (a-h) without pre-ionization after the maximum simulated time (a-d) and after 0.12 ns (e-h). The left half of each panel shows the electron density in uniformly distributed air n_0 and the right half in perturbed air n_{1-4} (Eq. 1). (i-l) Electron density in perturbed air with pre-ionization of $n_{e,0} = 10^{12}$ m^{-3} (left) and without pre-ionization (right).

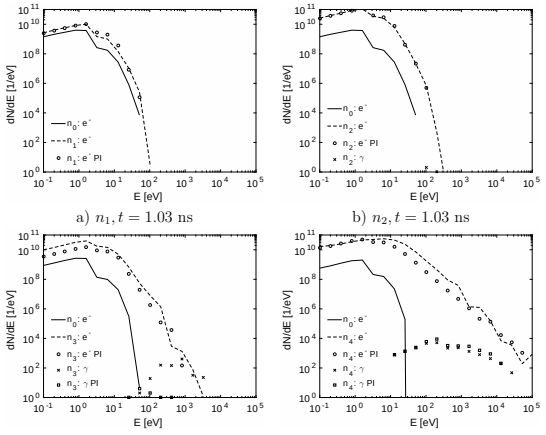

a) $n_1, t = 1.03$ ns b) $n_2, t = 1.03$ ns

c) $n_3, t = 0.37$ ns d) $n_4, t = 0.12$ ns

Figure 2. The energy distribution of electrons and bremsstrahlung photons for the time steps shown in Fig. 1. The electron energy distribution in uniform air density n_0 (solid), in perturbed air without pre-ionization $n_{j=1-4}$ (dashed) and with pre-ionization (circles). The photon energy distribution in perturbed air without pre-ionization ionization (crosses) and with pre-ionization (squares).